

Adaptive Scanning Optical Microscope (ASOM): A multidisciplinary optical microscope design for large field of view and high resolution imaging

Benjamin Potsaid, Yves Bellouard, and John T. Wen

Center for Automation Technologies, Rensselaer Polytechnic Institute, 110 8th Street,
Troy, New York 12180-3590

potsaid@alum.rpi.edu, y.bellouard@tue.nl, wenj@rpi.edu

Abstract: From micro-assembly to biological observation, the optical microscope remains one of the most important tools for observing below the threshold of the naked human eye. However, in its conventional form, it suffers from a trade-off between resolution and field of view. This paper presents a new optical microscope design that combines a high speed steering mirror, a custom designed scanner lens, a MEMS deformable mirror, and additional imaging optics to enlarge the field of view while preserving resolving power and operating at a high image acquisition rate. We describe the theory of operation and our design methodology, present a preliminary simulated design, and compare to existing technologies. A reduced functionality experimental prototype demonstrates both micro-assembly and biological observation tasks.

© 2005 Optical Society of America

OCIS codes: (010.1080) Adaptive optics; (110.0180) Microscopy; (150.3040) Industrial inspection; (170.1530) Cell analysis; (170.0110) Imaging systems; (170.3880) Medical and biological imaging; (170.0180) Microscopy; (170.5810) Scanning microscopy; (180.5810) Scanning microscopy; (220.1000) Aberration compensation; (220.3620) Lens design; (220.4830) Optical systems design.

References and links

1. B. Potsaid, Y. Bellouard, and J. T. Wen, "Scanning optical mosaic scope for micro-manipulation," in *Int. Workshop on Micro-Factories (IWMF02)*, R. Hollis and B. J. Nelson, eds., pp. 85–88 (2002).
2. M. Hafez, Y. Bellouard, T. Sidler, R. Clavel, and R.-P. Salathe, "Local annealing of shape memory alloys using laser scanning and computer vision," in *Laser Precision Microfabrication*, I. Miyamoto, K. Sugioka, and T. Sigmon, eds., Proc. SPIE **4088**, pp. 160–163 (2000).
3. W. Hardin, "Optical scanners enhance vision systems," *Vision Systems Design* **9**, 23–27 (2004).
4. H. Hoffer, L. Chen, G. Y. Yoon, B. Singer, Y. Yamauchi and D. R. Williams, "Improvement in retinal image quality with dynamic correction of the eye's aberrations," *Opt. Express* **8**, 631–543 (2001), <http://www.opticsexpress.org/abstract.cfm?URI=OPEX-8-11-631>.
5. M. J. Booth, M. A. A. Neil, R. Juskaitis, and T. Wilson, "Adaptive aberration correction in a confocal microscope," *Proc. Nat. Acad. Sci.* **35** 5788-5792 (2002)
6. B. Potsaid, Y. Bellouard, and J. T. Wen, "Design of an adaptive scanning optical microscope for simultaneous wide field of view and high resolution," in *Proceedings of IEEE International Conference on Robotics and Automation (Institute of Electrical and Electronics Engineers, New York, 2005)*, pp. 462–467.
7. W. J. Smith, *Modern Lens Design, Second Edition* (McGraw-Hill, 2005).

8. E. Hecht, *Optics*, 4th ed. (Addison Wesley, 2001).
9. D. B. Murphy, *Fundamentals of Light Microscopy* (Wiley-Liss, Inc., 2001).
10. R. S. Weinstein, M. R. Descour, *et al.*, "An array microscope for ultrarapid virtual slide processing and telepathology. Design, fabrication, and validation study," *Hum. Pathol.* **35**, 1303–1314 (2004).
11. J. Zemek, C. Monks, and B. Freiberg, "Discovery through automation," *Biophotonics International* **10**, 54–57 (2003).
12. C. Guestrin, F. Cozman, and S. Godoy, "Industrial applications of image mosaicing and stabilization," in *Proceedings of IEEE International Conference on Knowledge-Based Intelligent Electronic Systems (Institute of Electrical and Electronics Engineers, New York, 1998)*, vol. 2, pp. 174–183.
13. J. M. Rodgers, "Curved Focal Surfaces: Design Optimization Through Symmetry, Not Complexity," *Photonics Tech Briefs - Online* (2003), <http://www.ptbmagazine.com/content/040103ora.html>.
14. T. Fusco, J.-M. Conan, V. Michau, G. Rouseet, and F. Assemat, "Multi-conjugate adaptive optics: comparison of phase reconstruction approaches for large field of view," in *Atmospheric Propagation, Adaptive Systems, and Laser Radar Technology for Remote Sensing.*, J. D. Gonglewski, G. W. Kamerman, A. Kohnle, U. Schreiber, and C. Werner, eds., *Proc. SPIE* **4167**, pp. 168–179 (2001).
15. J. W. Hardy, *Adaptive Optics for Astronomical Telescopes* (Oxford University Press, 1998).
16. D. Wick, T. Martinez, S. Restaino, and B. Stone, "Foveated imaging demonstration," *Opt. Express* **10**, 60–65 (2002), <http://www.opticsexpress.org/abstract.cfm?URI=OPEX-10-1-60>.
17. L. Sherman, O. Albert, C. Schmidt, G. Vdovin, G. Mourou, and T. Norris, "Adaptive compensation of aberrations in ultrafast 3D microscopy using a deformable mirror," in *Three-Dimensional and Multidimensional Microscopy: Image Acquisition and Processing VII*, *Proc. SPIE* **3919**, pp. 9–13 (2000).
18. S. Kodiyalam and J. Sobieszczanski-Sobieski, "Multidisciplinary Design Optimisation - some formal methods, framework requirements, and application to vehicular design," *Int. J. Vehicle Design* **25**, 3–22 (2001).
19. B. Potsaid and J. T. Wen, "High performance motion tracking control," in *Proceedings of IEEE Conference on Control Applications (Institute of Electrical and Electronics Engineers, New York, 2004)*, pp. 718–723.
20. T. Bifano, J. Perreault, P. Bierden, and C. Dimas, "Micromachined deformable mirrors for adaptive optics," in *High-resolution wavefront control: methods, devices, and applications IV*, *Proc. SPIE* **4825**, pp. 10–13 (2002).
21. H. Zhang, Y. Bellouard, E. Burder, R. Clavel, A.-N. Poo, and D. W. Huttmacher, "Shape memory alloy microgripper for robotic microassembly of tissue engineering scaffolds," in *Proceedings of IEEE International Conference on Robotics and Automation (Institute of Electrical and Electronics Engineers, New York, 2004)*, pp. 4918–4924 (2004).
22. F. Ianzini, L. Bresnahan, L. Wang, K. Anderson, and M. Mackey, "The large scale digital cell analysis system and its use in the quantitative analysis of cell populations," in *Proceedings of 2nd IEEE-EMB Conference on Microtechnologies in Medicine & Biology (Institute of Electrical and Electronics Engineers, New York, 2002)*, pp. 469–475.

1. Introduction

Along with the recent growth of biotechnology and micro-electro-mechanical systems (MEMS), as well as an industrial trend towards miniaturization, there is a growing need to observe, interact with, and inspect at a scale below the threshold of the naked human eye. Fulfilling this need, the optical microscope has seen a resurgence of interest and will continue to be a critical tool as these fields advance. However, the essential optical design and operating principle has not changed significantly in the last century, and the optical microscope still suffers from a well known inherent tradeoff between the field of view and resolving power of the imaging system. This paper seeks to show that our new Adaptive Scanning Optical Microscope (ASOM) concept can effectively address this tradeoff and offers certain other advantages over the current state of the art. We achieve an expanded field of view at high resolution by integrating active optical elements, motion control, and image processing techniques with traditional static optical elements in a tightly integrated fashion.

The motivation for expanding the field of view initially came from our experiences in micro-assembly and precision manufacturing. Vision guided micro-assembly often requires the near-simultaneous monitoring of widely separated part features at micron to sub-micron level resolution (e.g. monitoring multiple critical edges of a micro-mirror and optical sensor being assembled onto a substrate). Because a single microscope can't offer an adequately large field of view at the required resolution, multiple microscopes and/or a moving stage provide a readily available off-the-shelf solution. However, the limitation in movements per second and agitation

of the specimen due to the moving stage, and considerable effort required to reposition and calibrate multiple microscopes for each new assembly task suggested the need for a new optical microscope design to address these issues. For the same reasons, such a microscope would also be desirable for biological and medical imaging. Our first design [1], called the Scanning Optical Mosaic Scope (SOMS), was constructed to demonstrate the advantages of combining a high speed post-objective scanning system with real-time mosaic constructing techniques for use in micro-assembly and biological imaging. The optical layout was originally inspired by a machine created at EPFL for laser annealing shape memory alloy [2] and shares the concept of a post-objective 2-D scanning mirror. This configuration is also used in several commercial products [3], but in its basic form, has a limited field of view because of off-axis aberrations in the scanner lens.

The ASOM design we discuss in detail for the first time in this paper (the basic ASOM concept was first presented at the ICRA conference in 2005 [6]) shares the scanning and mosaic construction principle of the SOMS. However, the ASOM differs from existing technologies in that it incorporates a deformable mirror to address off-axis aberrations introduced by a custom designed scanner lens that allows for up to several waves of aberration. Additionally, the scanner lens is simplified by relaxing the flat field requirement and works with the steering mirror to project a significantly curved intermediate image field that rotates about its own center. The underlying concept of the ASOM is to use a low mass and very fast steering mirror located between the scanner lens and the imaging optics to form a post-objective scanning configuration. An image is acquired at each scan position, and through image mosaic techniques, a large composite image of the object can be rapidly constructed. The advantages of such an arrangement are: a large effective field of view at high resolution, no disturbance to the sample, and the ability to achieve many movements/images per second. However, such a system configuration also poses significant design and implementation challenges due to the off-axis imaging, which we address by:

1. Explicitly incorporating field curvature into the design to greatly reduce the complexity of the scanner lens.
2. Introducing an actuated deformable mirror (DM) into the optical path to correct for the residual aberrations that are scan position dependant.
3. Image processing to remove image distortion.

The ASOM design will excel in applications where critical spatial-temporal observations are demanded, but will not offer the virtually unlimited field of view associated with the moving stage. Biological applications where the ASOM would be attractive are: observing dynamic cellular events (mitosis, viral attachment, motility, cellular response to chemical application) over a large population of living cells or observation of select regions of interest on tissue samples. In industry, the ASOM will allow for vision guided micro-assembly and rapid inspection of completed parts, with the potential for higher product throughput.

In this paper, we first discuss wide field of view and high resolution imaging in Section 2. Section 3.1 describes the key features of the ASOM; Section 3.2 presents our initial design approach; and Section 3.3 presents simulated performance results. Finally, Section 4 describes our first experimental reduced functionality implementation with demonstrations in micro-assembly and biological observation.

2. Wide Field Optics and Imaging

The design of wide field and high resolution microscopic imaging systems are driven by consideration of (1) an image sampling issue and (2) an image quality issue. First, consider an

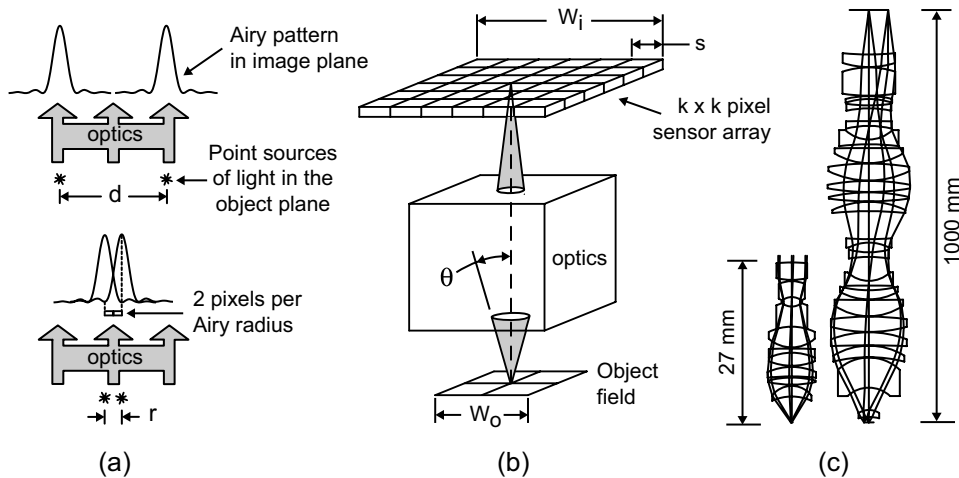


Fig. 1. (a) Optical systems image two point sources in the object plane as two Airy patterns in the image plane. Two pixels are required per Airy core radius to avoid aliasing the image. (b) Black box imaging system. (c) Microscope (left) and lithography lens (right). The lens prescriptions for the microscope objective and lithography lens were obtained from [7] and are not shown to scale.

imaging system with optics that are nearly perfect (i.e. the optical aberrations are much below the diffraction limit). Such a system will image two point sources separated by a distance, d , as two overlapping Airy patterns in the image field as shown in Fig. 1(a). As the distance between the two points decreases, a critical distance will be reached, r , where the two points can no longer be individually distinguished. According to the Rayleigh criteria, this critical distance, called the resolution, occurs when the center of one Airy disk falls on the first minimum of the other [8] and is related to the numerical aperture, NA, of the system and the wavelength of light, λ , by [9]:

$$r = \frac{0.61\lambda}{NA}, \quad (1)$$

where the NA of the system is defined by the index of refraction of the transmitting medium, n , and the half angle, θ , of the cone of light collected from the object: $NA = n \sin(\theta)$.

A digital camera must sample with two pixels per Airy core radius to avoid aliasing according to the Nyquist sampling criteria [9]. This observation provides the following maximum theoretical object field width, W_o , for a sensor array pixel count per edge, k , and resolution, r :

$$W_o = \frac{kr}{2}. \quad (2)$$

While microscopic imaging systems are often designed with resolutions in the $\frac{1}{4}\mu m$ to several μm range, the lower practical limit on CCD camera pixel size is approximately $6\mu m$ due to noise effects. Therefore, the optics must enlarge the Airy pattern to achieve proper sampling, with the required minimum magnification factor, M , for a given sensor pixel size, s is given by: $M = 2s/r$. At this critical magnification, the corresponding image size, W_i , is: $W_i = ks$. Fig. 1(b) illustrates the above mentioned equations and represents the imaging optics as a generic black box. The optical design task is to specify the design of the imaging system, i.e., to fill in the details of the black box with specific lens or mirror geometries, glass types, and spacing.

The first intuitive approach to designing a large field and high resolution imaging system might be to take an existing microscope layout, such as that shown in Fig. 1(c), and simply increase the pixel count of the camera while redesigning the optics to achieve a larger field of view. This approach may indeed be possible, but it is not generally practical as the requirements for field size, flat field, and numerical aperture soon approach those of lithography lenses. The 1998 Nikon lithography lens (US Patent 5,805,344) shown in Fig. 1(c) has a 0.65 NA with field sizes of 93.6mm and 23.4mm for the mask and wafer image respectively. Lithography lenses require near perfect manufacturing and extremely tight assembly tolerances (often requiring an interferometric assembly process), and can cost in the millions of dollars [7]. Also notice the presence of negatively powered elements located at the narrow beam regions in both the microscope and lithography lenses and positively powered elements where the beam is wide. This design technique is used to achieve a flat imaging field (small Petzval sum) and results in an increase in the lens count and optical complexity. An additional consideration is the size of the image sensor, given that large commercially available CCD cameras only have approximately 9216×9216 pixels (e.g. Fairchild Imaging CCD595). Smaller CCD arrays can be assembled into a mosaic to achieve larger pixel count with the advantage of being able to read data off the imaging chips in parallel (data rates for getting the image data off the chip can be the limiting factor determining maximum refresh rates), but at a cost of additional precision assembly requirements. Even with modern technology and manufacturing capabilities, a large field and high resolution imaging system based on a purely static optical design will only see limited application because of the exceedingly high cost, large size, tight assembly tolerances, and optical complexity.

Table 1. Qualitative comparison of ASOM to other technologies

	No specimen agitation during scanning	Preserves resolving power while expanding field of view	Easy manufacturing integration over conveyor transport	Scanning rate (movements or images per second)	Easily reconfigured for different viewing tasks
Multiple Parfocal Objectives	X			LOW	
Zoom Lens Design	X		X	MED	
Moving Stage		X		MED	X
Moving Microscope	X	X	X	LOW	X
Multiple Microscopes	X	X	X	HIGH	
Basic Post-Objective Scanning	X		X	HIGH	X
DMetrix	X	X		HIGH	
ASOM	X	X	X	HIGH	X

Some of the alternative modern approaches to address the field size and resolution tradeoff are summarized in Table 1. The first five methods (multiple parfocal objectives through multiple microscopes) are well established and quite common. In this table, the "basic post-objective scanning" method refers to the commercially available units [3], which are limited to very low numerical aperture and suffer from considerable off-axis aberration because of the system

layout. Of particular interest is the array microscope sold by DMetrix [10]. This system uses an array of 80 miniature microscopes (each of 3 element aspheric design) working in parallel to rapidly acquire the image. By slowly advancing the microscope array along the length of a microscope slide, a large composite image can be constructed. Given the parallel imaging paths, this is the fastest area scanning technology producing medical diagnostic grade images of static objects that the authors are aware of at this time (scanning, compressing, and storing an area of 225mm^2 at 0.47 microns per pixel in 58 seconds).

With parallel image acquisition and a relatively slow re-positioning speed, the DMetrix excels at static and high fill factor applications. Because the ASOM acquires images serially in time with extremely fast re-positioning speeds, the ASOM will excel in dynamic and/or low fill factor applications. Low fill factor applications include biological imaging of rare events over a large cell population, tracking multiple moving organisms, medical diagnostics of tissue sampled by needle extraction which is haphazardly placed on a microscope slide, etc. Most manufacturing applications require a low fill factor as only certain critical regions need to be observed or inspected with dynamic tracking of objects or features often required during assembly. More generally, the ASOM is particularly suitable for challenging spatial-temporal observation tasks requiring both a wide field of view and high resolution. Consideration of these issues motivated and contributed to the design of the ASOM.

3. ASOM Concept, Design, and Simulated Performance

3.1. Theory of operation

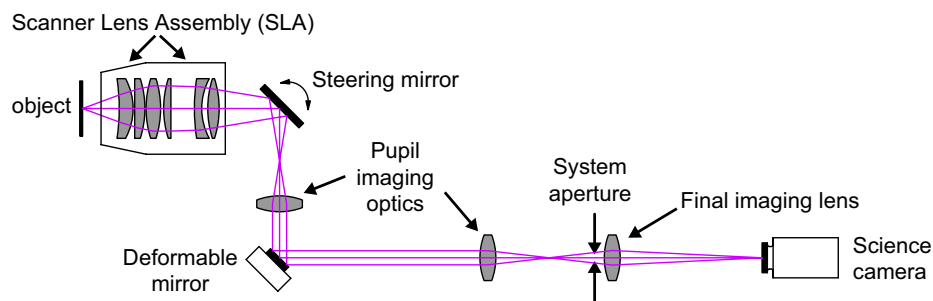


Fig. 2. Conceptual layout of the ASOM

The ASOM operates by taking a sequence of small spatially displaced images in rapid succession and then assembling a large composite image (mosaic) of the scene. The concept of expanding the field of view while preserving resolving power through mosaic construction is well established and has long been applied to biological imaging [11] as well as industrial imaging [12]. However, instead of a moving stage as is common, the mechanism and scanning principle in the ASOM consists of a high speed 2-D steering mirror working in coordination with a specially designed scanner lens assembly, a deformable mirror, and additional imaging optics. A conceptual layout of the ASOM is shown in Fig. 2.

Figure 3 shows the conjugate image and aperture planes of the ASOM system and partitions the optical elements into a scanner lens, forward eye-piece, inverted eye-piece, and final imaging optics. The scanner lens collects light from the object while the steering mirror, located at an image of the pupil, aims a projected real intermediate image. Acting like a conventional eye-piece in a traditional microscope, the forward eye-piece in the ASOM samples the first intermediate image and projects an external pupil to where the deformable mirror is located. The forward eye-piece in our preliminary design resembles a Huygens' eyepiece in that the in-

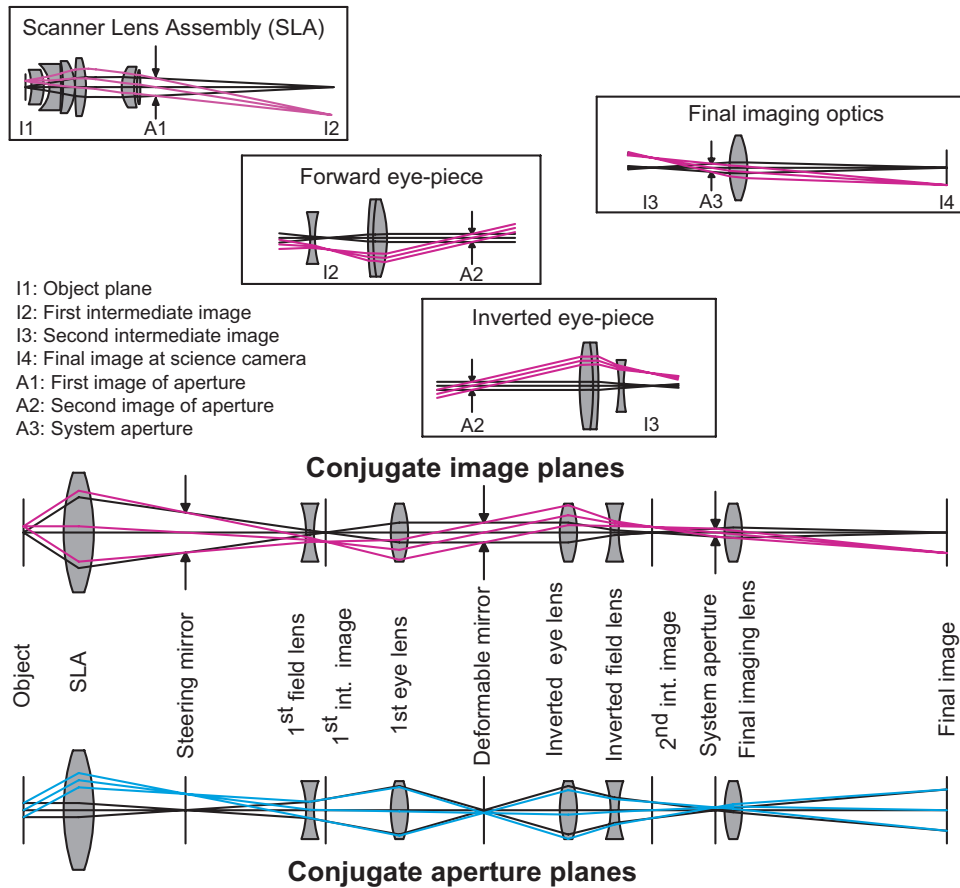


Fig. 3. Conjugate image and aperture planes

intermediate image is located between the field-lens and eye-lens. A notable difference is the use of a negative field lens. This has the effect of lengthening the deformable mirror relief (distance between eye-lens and deformable mirror), but at a cost of a larger eye-lens [7]. The inverted eye-piece resembles a Kellner eye-piece, but has a negative field lens. The negative field lenses also help contribute to a negative Petzval sum in the imaging optics. The final imaging optics relay the second intermediate image to the science camera with the proper magnification to prevent aliasing and also contain the true system aperture stop.

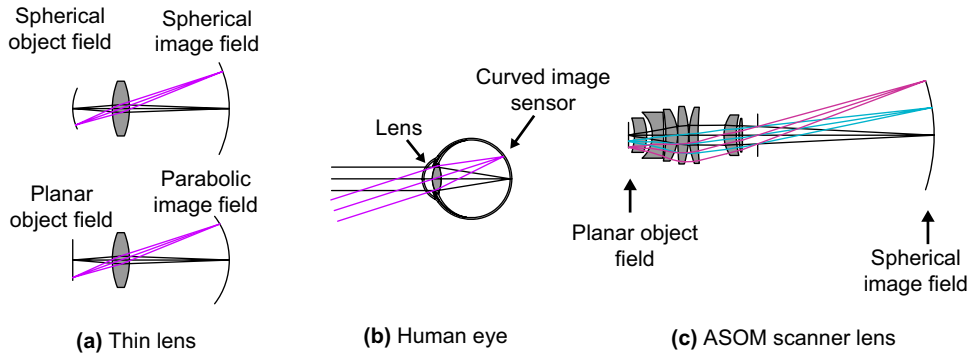


Fig. 4. (a) Shape of image field for a thin lens (b) The curved surface of the retina (image sensor) allows for a very simple lens in the human eye (c) The ASOM scanner lens is simplified by allowing a curved image field

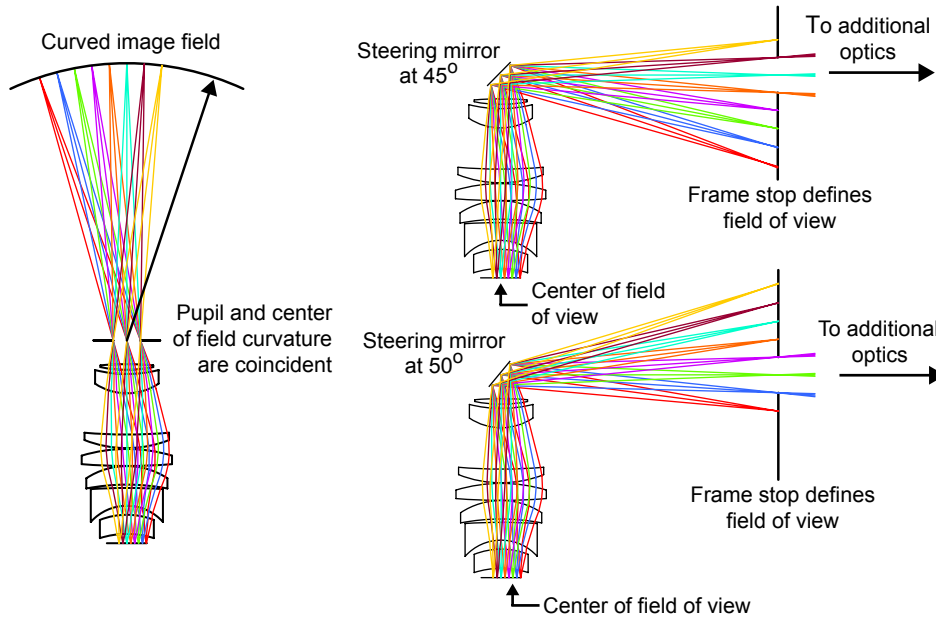


Fig. 5. Curved image field of scanner lens assembly

Curved field scanning layout - Different than a microscope objective or lithography lens, the scanner lens on the ASOM is designed to exhibit significant field curvature with a relatively large Petzval sum. This relaxation of the flat field requirement offers the advantage of a greatly simplified optical design with far fewer lens elements, as the "natural" behavior of a lens is to image with a curved image field as shown in Fig. 4. Because positive lens elements contribute positive Petzval sum and negative lens elements contribute negative Petzval sum, the design of flat field imaging systems requires careful use of both positive and negative lens elements to achieve a near zero system wide Petzval sum. Non-unity magnification is obtained by placing the negative lens elements at narrow beam diameter regions and positive lens elements at wide

beam diameter regions. Compare the relatively simple ASOM scanner lens that allows for a curved image field as shown in Fig. 4 to the flat field microscope objective and lithography lens shown in Fig. 2. Also note that the advantages of curved field designs have been recognized for aerospace applications [13], offering considerable weight savings and design simplicity.

Additional important characteristics of the ASOM scanning system that are not typical optical design goals include:

1. The center of the field curvature, the rotation center for the 2-D steering mirror, the mirror surface, and an optical pupil plane are all mutually coincident.
2. The shape of the projected image surface is nearly spherical instead of the more typical parabolic surface associated with field curvature. This is achieved through higher order aberration control.

Under the above mentioned conditions, as the steering mirror angle changes, the projected curved image surface rotates about its own center as shown in Fig. 5. Stationary imaging optics with a matching negatively curved imaging field work with a frame stop to sample a portion of the image surface, providing for an image scanning and selection mechanism as the steering mirror angle changes.

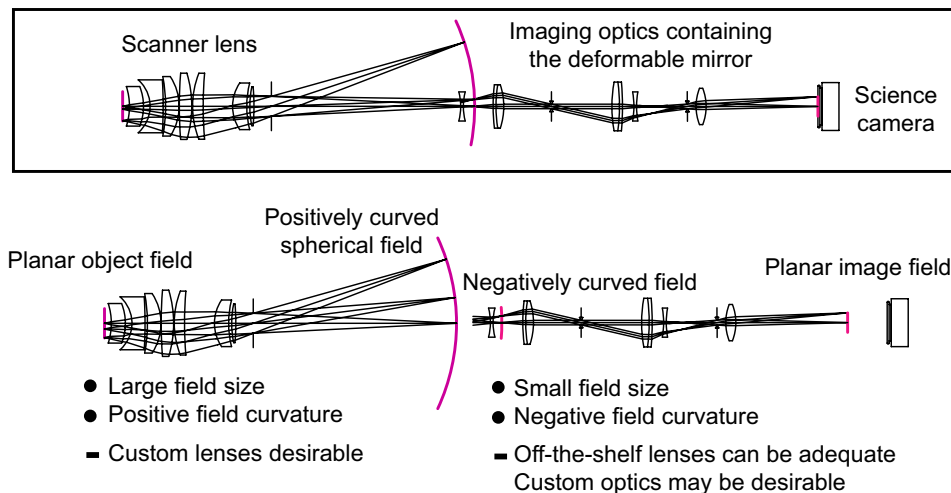


Fig. 6. Field curvature of scanner lens assembly and imaging optics

This layout is advantageous because it eliminates the need for a large *and* flat field imaging system. Instead, as shown in Fig. 6, the system exhibits (1) a large positively curved field associated with the scanner lens, and (2) a small negatively curved field associated with the imaging optics, thus avoiding the significant difficulty of designing and manufacturing a large continuous flat field imaging system as discussed in Section 2. In fact, because the *imaging optics* are low numerical aperture, small field size, and used predominantly on-axis, we have found that off-the-shelf optics can provide sufficient aberration correction for diffraction limited performance when used with medium size sensor arrays (512×512 pixels). Larger sensor arrays may require custom imaging optics.

Deformable mirror wavefront correction - While the scanner lens and overall system layout are explicitly designed to manage field curvature, other off-axis aberrations (e.g. coma, astigmatism, and other higher order aberrations) are still present. The traditional solution would be

to add lens elements to balance the residual aberrations, but with such extreme off-axis imaging as performed in the ASOM, a fully compensated lens assembly would require a prohibitively large lens count. We circumvent this problem by designing a "good" scanner lens with significant wavefront aberration (up to several waves of optical path difference), and then use a deformable mirror to compensate for the aberrations over the specific viewing field that is selected. Variation in the aberration is allowed between individual field positions throughout the scanner's range. However, given that the deformable mirror can only achieve one specific shape at a time, the rate of change in the aberration between field positions must be small enough to allow diffraction limited imaging performance over the entire sub-field of view that is selected. This is similar to the concept of the isoplanatic patch in the atmosphere [15] that is widely recognized in the adaptive optics telescope community. By analogy with the ASOM, the isoplanatic patch of the scanner lens must be larger than the selected sub-field of view. Otherwise, the image may blur at the edges of each sub-field of view.

An adaptive optics technology, deformable mirrors have been used to allow for high resolution imaging inside the human eye [4], which is particularly challenging because of the time varying aberrations of the eye's lens. Similarly, deformable mirrors have also been used to correct for off-axis aberrations and sample induced wavefront disturbances in confocal microscopy [5, 17]. Expanding the field of view in imaging systems has also previously been shown with a liquid crystal spatial light modulator to create a foveated imaging system [16].

3.2. Design process

Modern optical design is generally performed using the simulation and optimization capabilities of commercially available lens design software, such as ZEMAX, CODE V, or OSLO. Local minima searching algorithms can often improve an initial design, but are highly dependant on the starting values of the design variables and often get caught in a local minima [7]. For this reason, a global search is often performed first to explore a large design space [7]. Applied directly to the ASOM design problem, the ZEMAX genetic algorithm (global search) proved ineffective because of the size (number of design variables) and complexity of the system (requires multiple configurations to accommodate the different mirror angles and DM shapes required for each field position). Instead of an all-in-one global optimization approach, we partitioned the system into (1) a scanner lens assembly and (2) the imaging and wavefront correcting optics as shown in Fig. 6. The scanner lens assembly was designed as a fully static system (no moving elements) for a curved field with up to several waves of aberration (with the assumption that the deformable mirror would eventually correct for this aberration). The imaging and wavefront correcting optics were then designed separately for diffraction limited performance over the entire field with the deformable mirror held flat. The compatibility at the interface of the two subsystems with respect to field curvature radius, NA, and subsystem magnification was maintained by human intervention, much trial and error, and many design iterations. Once consistency between the two subsystems was nearly achieved, the two subsystems were joined with the steering mirror and deformable mirror added to the system. The local optimization algorithm and the multi-configuration capabilities of ZEMAX allowed for the system wide optimization of the lens geometries and spacing while simultaneously considering multiple field positions, steering mirror angles, and specific deformable mirror shapes. Future work will investigate more formal and automated design approaches and, like the existing design methodology developed for the ASOM that was used to synthesize the simulated design presented in this paper, will draw heavily from the field of Multidisciplinary Design Optimization (MDO) [18].

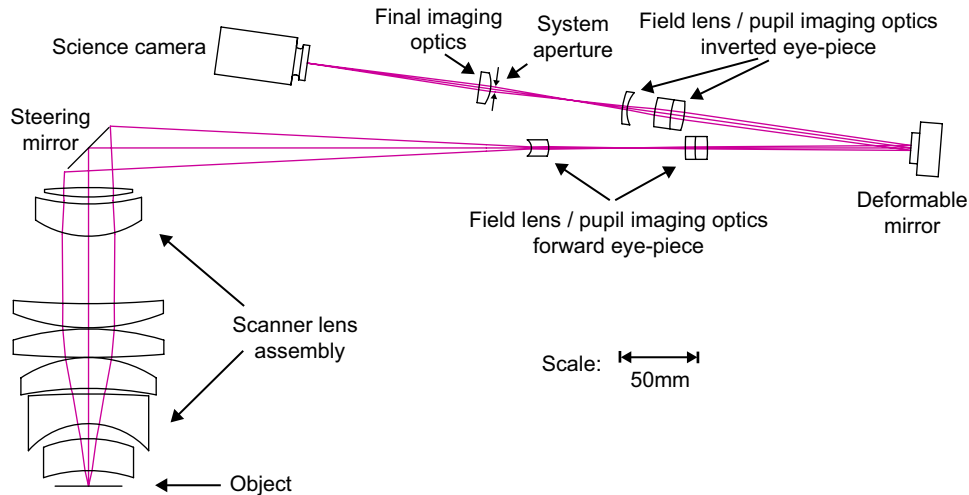


Fig. 7. ASOM preliminary design

3.3. Specifications and predicted performance

A practical design resulting from the optimization described in Section 3.2 is shown in Fig. 7. The simulated results that follow demonstrate that the ASOM can effectively provide an expanded field of view while preserving resolution when compared to existing microscope technologies. Table 2 lists performance specifications of the specific ASOM design described in this paper, but with suitable changes to the design, the field area and numerical aperture could be tailored to the observation task at hand. However, in general, as the field area increases, the realizable NA will decrease due to physical and practical limitations.

Table 2. Preliminary ASOM performance specifications

	Specification
Effective field of view diameter	40mm
Total observable field area	1257 mm ²
Numerical aperture	0.21
Operating Wavelength	510 nm
Resolution	1.5 μm
Magnification	15.2
Camera pixel count	512 × 512
Camera pixel size	10μm

Figure 8 compares the observable field of view of the ASOM to a fixed microscope with a 4096 × 4096 camera (considered a full field camera with standard microscope objectives) and with a 1024 × 1024 camera, which is more common. The ASOM offers diffraction limited (Strehl ratio > 0.8) for all field positions based on high fidelity simulation. The field sizes for the fixed microscope designs assume perfect imaging and were calculated using Equations 1 and 2 using a 0.21 numerical aperture with $\lambda = 0.510\mu\text{m}$ for the wavelength of light (green light is relatively nondestructive and desirable for imaging living biological cells).

Also shown in Fig. 8 is the sub-field of view offered by the 512 × 512 camera used in this ASOM implementation. In this design, the relatively simple imaging optics limit the camera

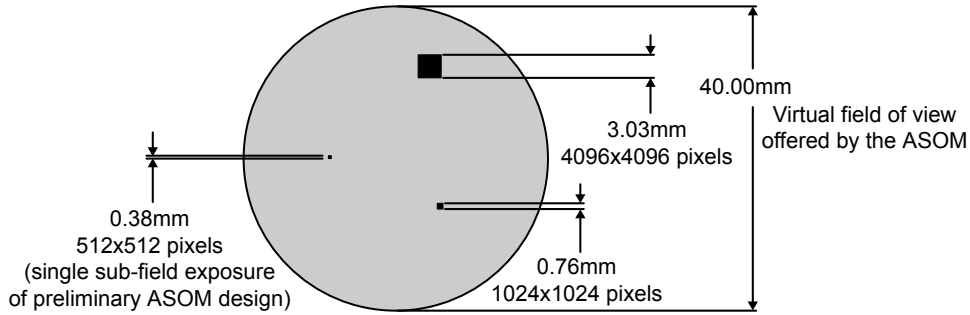


Fig. 8. The 40mm virtual field of view of the ASOM is compared to that offered by a traditional microscope using a 1024×1024 and 4096×4096 camera (all systems operating at 0.21 NA). The 0.38mm size of the ASOM sub-field of view is also shown with a 512×512 camera, requiring many scan movements to cover the entire 40mm field.

sensor size to be about 6.0mm in diameter for diffraction limited performance. With a suitable redesign of the imaging optics, the diffraction limited field size of the imaging optics could be enlarged to use a higher pixel count camera. Nevertheless, even with the small 512×512 camera, the scan times listed in Table 3 are competitive with existing technologies. The table presents the estimated scan time for 100, 250, and 500 frames per second camera rate and for 100%, 50%, and 10% fill factors. These calculations assume that the total number of scan movements is given by: number of scans = total effective field area / sub-field area. Based on our previous work with high speed steering mirrors [19], we estimate that we can achieve at least 100 movements per second.

Table 3. Estimated scan times (sec.) for different camera pixel counts and scan rates

Camera frame rate:	100 fps			250 fps			500 fps		
Fill factor (%):	100	50	10	100	50	10	100	50	10
512×512 pixels	87	44	8.7	35	17	3.50	17	8.74	1.7
1024×1024 pixels	22	11	2.2	8.7	4.4	0.87	4.4	2.18	0.44
4096×4096 pixels	1.4	0.68	0.14	0.55	0.27	0.054	0.27	0.14	0.027

We next demonstrate the wavefront correcting capabilities of the deformable mirror. The μ DM100 DM from Boston Micromachines with 100 electrostatic actuators, a 3.3mm round aperture, and $2\mu\text{m}$ stroke was chosen for this design [20]. Instead of modeling all 100 actuators, we created a user defined surface in ZEMAX consisting of a set of 43 evenly spaced Gaussian basis functions to represent the mirror surface shape. We assume that the surface generated with the low spatial frequency Gaussian shapes can be reproduced by the deformable mirror within the maximum actuator stroke (this will soon be verified by finite element analysis). The amplitude of each basis function becomes a variable in ZEMAX and can be optimized with the other glass geometry and spacing variables as well as the steering mirror angle.

Figure 9 shows how the DM corrects for the specific wavefront aberration associated with each field position. Over the entire field and for all field positions, the Strehl ratio is much greater than the diffraction limit of 0.8, resulting in near perfect imaging.

All results presented here are based on idealized simulations ignoring the reality that lenses and optical housings are always subject to manufacturing and assembly tolerances. We will consider these aspects in future work.

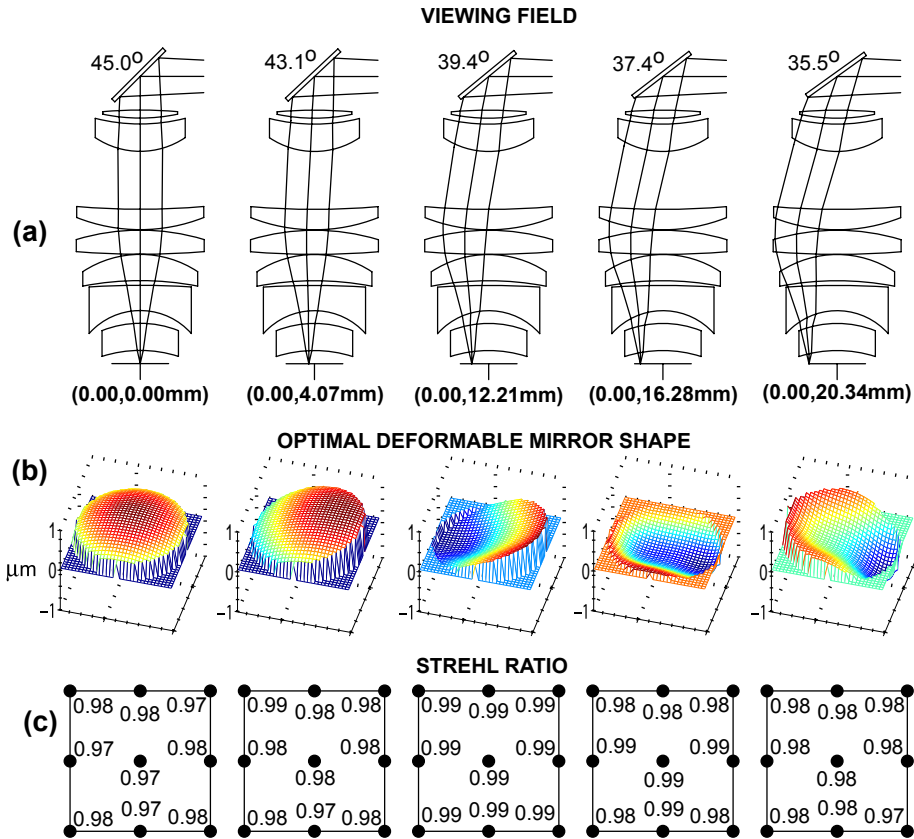


Fig. 9. (a) Viewing different field positions (b) Optimal deformable mirror shape for the specific field position (c) Strehl ratio sampled over the selected field of view

4. Experimental Prototype and Demonstrations

4.1. Experimental hardware

To demonstrate the basic principle of scanning and image mosaic construction, we have built a first generation prototype [1] called the Scanning Optical Mosaic Scope (SOMS). No formal optimization of this design was performed, and the prototype unit was constructed using standard catalog lenses available from ThorLabs, a Sony XC-77BB CCD camera, Matrox Meteor II frame grabber, Cambridge technologies galvanometers and servo drivers, and a TI based DSP board. It differs from the more advanced ASOM design proposed in this research in that: (1) the optical layout is simplified, (2) there is no deformable mirror or adaptive optics, (3) all lenses are available as standard catalog items, (4) the scanner lens is a single standard achromat doublet.

4.2. Micro-assembly and biological demonstrations

The micro-manipulation demonstration is based on a shape memory alloy microgripper [21] moving between two fixed objects in a workspace. A rudimentary correlation based image matching algorithm and Kalman filter are used to track the motion of the gripper tip. A 3×3 tile mosaic images the gripper and the scanning pattern is automatically adjusted to maintain the gripper tip in the center tile. The scan pattern also includes the two stationary objects in

the workspace, demonstrating the capability of the SOMS to observe multiple stationary and moving objects in the workspace nearly simultaneously. A sequence of the video footage is shown in Fig. 10.

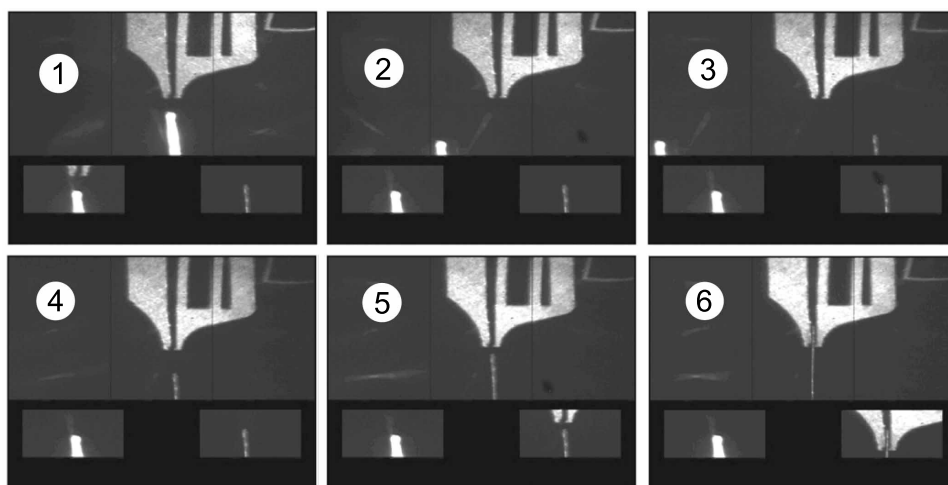


Fig. 10. (774 KB, 14 MB version) Movie demonstrating microgripper tracking with a 3x3 tile mosaic while simultaneously monitoring 2 fixed objects in the workspace.

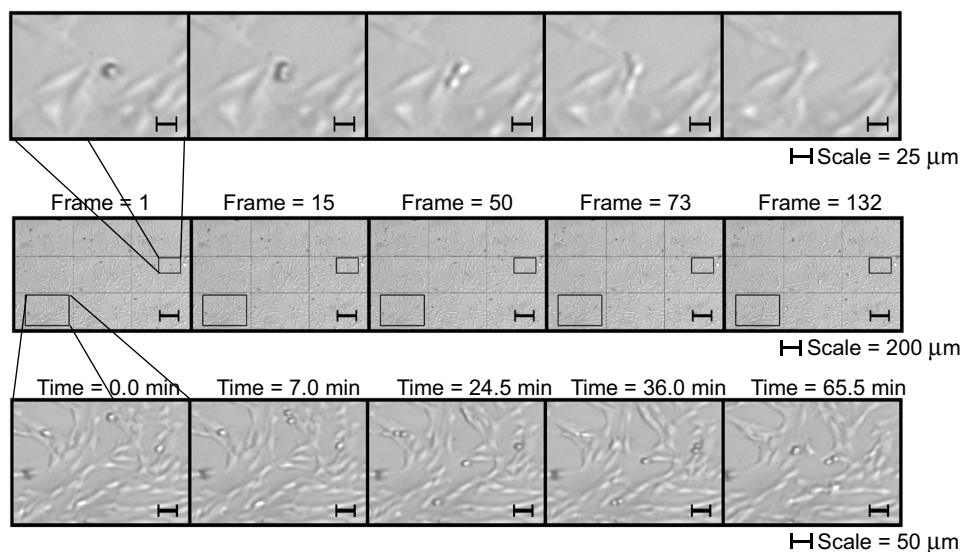


Fig. 11. (1.13 MB, 14 MB version) Movie showing a 3X3 mosaic of living cells taken with the SOMS.

Figure 11 shows a video sequence of living biological cells (Telomerase-Immortalized hTERT-RPE1). A 3 × 3 tile image mosaic monitors a large cell population without disturbing the cells, which are kept alive in a temperature regulated nutrient solution. Several events of mitosis (cell division) can be seen occurring throughout the viewing field. The ASOM not only offers the possibility of automatically detecting the onset of mitosis and other events, but can

be easily programmed to track and record multiple events at the same time. While automated quantitative cell analysis using a moving stage has recently been proposed [22], the bandwidth of the overall system is still constrained by the response of the stage and the sensitivity of the cell specimen to motion. The ASOM will address both of these issues.

5. Conclusion

We have presented a new microscope concept that can simultaneously achieve high resolution and a large effective field of view that offers several advantages over the current state of the art for observing certain spatial-temporal events. The design draws heavily on the synergy of an optical, mechanical, motion control, and image processing design. ZEMAX optical simulations show diffraction limited imaging performance over a greatly enlarged field of view, while calculations show the possibility for high speed movement and image acquisition operation. A reduced functionality proof-of-concept prototype has been constructed to demonstrate the basic efficacy of the mirror based scanning approach and we demonstrate with both micro-assembly and biological observation tasks.

The next generation ASOM experimental hardware that we are now building will be fully functional, include a deformable mirror, and will demonstrate all aspects of the ASOM design as presented in this paper. However, considering the high cost and lead time of the custom optics, this next generation ASOM will use off the shelf optics exclusively. A consequence of this additional constraint is that the NA and the field size will be smaller than the design presented in this paper. The calibration and online optimization of the active optical elements is a significant challenge and will be a focus of future work. Meanwhile, we continue to develop a systematic design optimization and have started to consider manufacturing errors and assembly tolerances in the design.

Acknowledgments

The authors would like to thank Richard Cole at the Wadsworth Center, New York State Department of Health and Dr. Jacques Izard at the Forsyth Institute. Their expertise and knowledge of microscopy and cellular processes have contributed greatly to the project. This research is also supported in part by the Center for Automation Technologies under a block grant from the New York State Office of Science, Technology and Academic Research (NYSTAR).